

Supplementary Information:

Photo-induced radical polarization and liquid-state dynamic nuclear polarization with fullerene nitroxide derivatives

Guoquan Liu, Shu-hao Liou, Nikolay Enkin, Igor Tkach and Marina Bennati

Max-Planck Institute for Biophysical Chemistry, Am Faßberg 11, 37077 Göttingen, Germany; and Department of Chemistry, University of Göttingen, Tammanstr. 2, 37077 Göttingen, Germany

Section S1: Field-dependent CW transient EPR of FN derivatives and C₆₀

Section S2: UV-Vis spectrum of C₆₀, FN and its derivatives and extinction coefficients

Section S3: Estimation of $\alpha(^3\text{C}_{60})$ from the extinction coefficient and laser pulse power

Section S4: FID intensities of the DNP ¹H-NMR measurements and pulse sequence

Section S1: Field-dependent CW transient EPR of FN derivatives and C₆₀

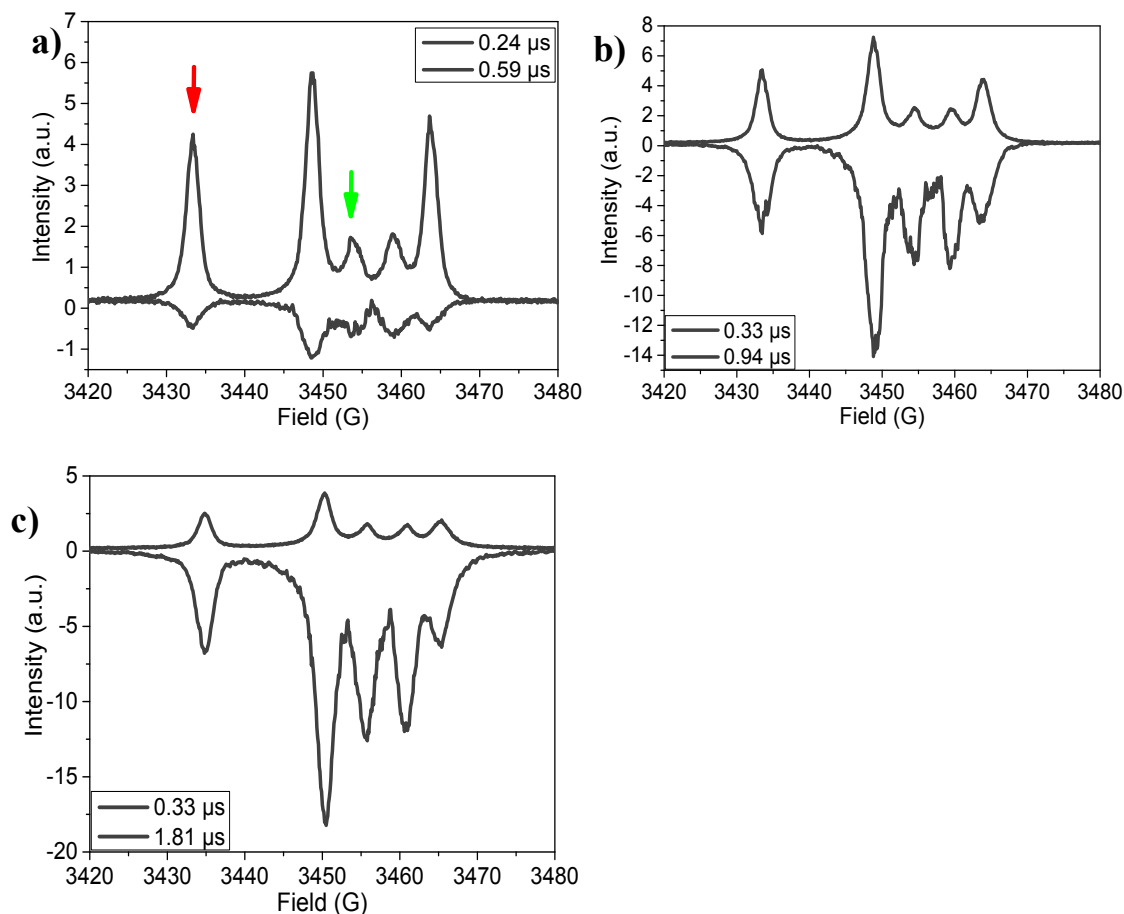


Figure S1. Field-dependent CW transient X-band (9.8 GHz) EPR signals of the **FN** (a) and its derivatives **FN-1a** (b) and **FN-2a** (c) after laser pulse at 532 nm. Representative transient EPR spectra at two different time delays as indicated in the legends, showing the initial emissive and then absorptive signals. Arrows in (a) mark the positions of the transients recorded on Fig. 2A of the main text. Microwave power was 2 mW ($B_1 \approx 0.064$ G, $\omega_1/2\pi \approx 0.2$ MHz), laser pulse energy is approximately 2 mJ.

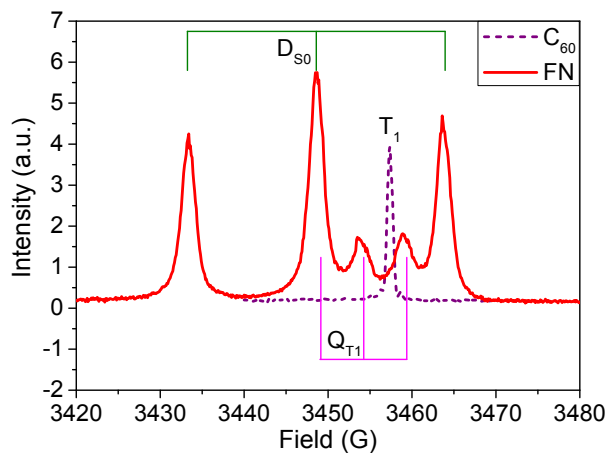


Figure S2. CW transient EPR spectrum of **FN** and **C₆₀** at X-band at time delay of 0.59 μ s after laser pulse, respectively.

Section S2: UV-Vis spectra of C₆₀, FN and its derivatives and extinction coefficients

Optical absorption spectra of C₆₀ and FN derivatives are displayed in Fig. S3. The extinction coefficients at 532 nm were determined according to the Beer–Lambert law using three samples of known concentrations. The experimental results are listed in Tables S1 and S2. The value of C₆₀ is in good agreement with literature values ($\epsilon_{532}(\text{C}_{60}) = 750\text{--}900 \text{ M}^{-1} \text{ cm}^{-1}$, depending on different solvents).[1] The value for FN is in best agreement with the value of Ref. 2.[2]

Table S1. Concentrations of C₆₀, FN, FN-1a and FN-2a and its corresponding absorptions at 532 nm in toluene.

[C ₆₀](mM)	Abs.	[FN](mM)	Abs.	[FN-1a](mM)	Abs.	[FN-2a](mM)	Abs.
0.1	0.091	0.04	0.058	0.05	0.104	0.02	0.084
0.2	0.181	0.1	0.141	0.1	0.196	0.1	0.318
1.0	0.97	0.65	0.782	0.2	0.431	0.25	0.754

Table S2. Extinction coefficients of the various molecules in toluene at 532nm. Error is estimated up to 20 %.

sample	$\epsilon (\text{M}^{-1} \text{ cm}^{-1})$
C ₆₀	900
FN	1200
FN-1a	2200
FN-2a	2900

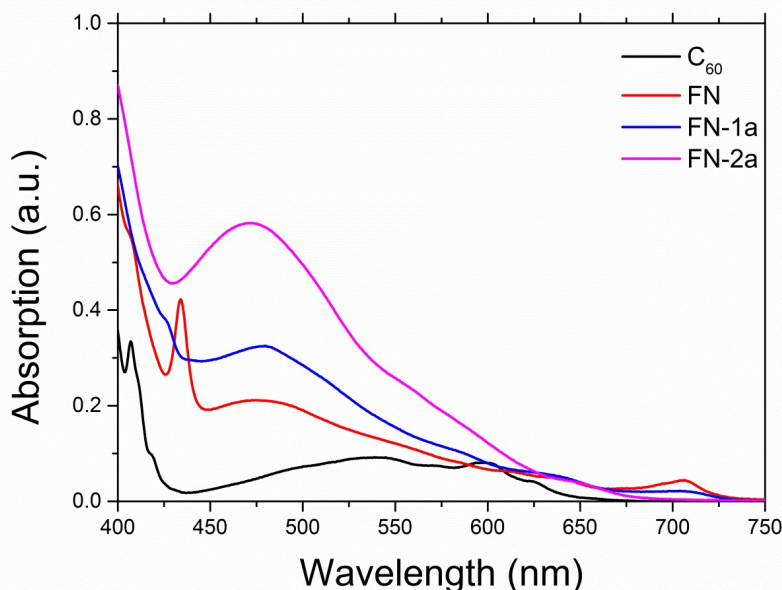


Figure S3. UV/Vis spectra of C₆₀ (black), FN (red), FN-1a (blue) and FN-2a (purple). The concentration of each sample was 0.1 mM, sample was loaded into a cuvette with 1 cm light path. All spectra were collected using a Varian CARY100 UV-Vis spectrometer.

Section S3: Estimation of $\alpha(^3C_{60})$ from the extinction coefficient and laser pulse power

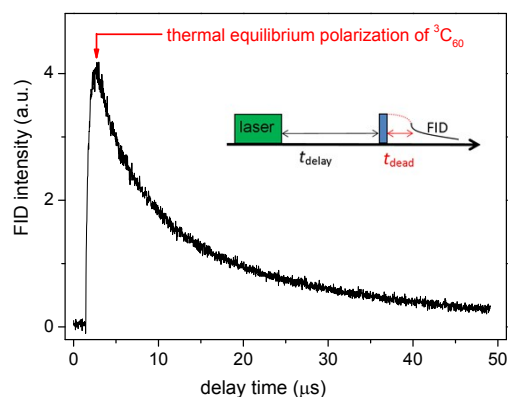


Figure S4. Time evolution of the FID intensity (X-band) of the photo-excited $^3C_{60}$ after a laser pulse. Sample was in toluene solution (1.6 mM, 20 μ L). Experiment conditions: dead time (t_{dead}) 200 ns; $\pi/2$ -mw pulse length 20 ns; laser wavelength 532 nm; laser pulse energy 2 mJ.

Table S3. FID intensities of 4-oxo-TEMPO- d_{16} - ^{15}N in toluene at three different concentrations. Sample volume was 20 μ L, laser illumination (4 mJ/pulse) was applied to maintain similar experimental conditions as the measurements in Table S4. EPR detection was set at the low-field nitroxide hyperfine transition.

concentration $c(NO)$ (mM)	$I^{det}(NO)$ at $t_{delay} + t_{dead}$ (a.u.)	$T_{2,NO}$ (ns)	t_{dead} (ns)	video gain	$I(NO)$ at 36dB video gain (a.u.)
2.6	1.2×10^4	100	100	30	6.5×10^4
1.4	1.1×10^4	140	100	30	4.5×10^4
0.8	1.2×10^4	200	100	36	2.0×10^4

Table S4. Estimation of $\alpha(^3C_{60})$ for samples at different concentrations and laser energy. The error is approx. 20%. Experimental conditions: sample volume 20 μ L; video gain 36dB.

concentration $c(C_{60})$ (mM)	laser energy (mJ/pulse)	$I^{det}(^3C_{60})$ at $t_{delay} + t_{dead}$ (a.u.)	$T_{2,^3C_{60}}$ (ns)	t_{dead} (ns)	$I(^3C_{60})$ at $t = 0$ (a.u.)	$\alpha(^3C_{60})$
1	4	9.7×10^3	440	100	1.2×10^4	0.08
0.5	4	5.8×10^3	430	100	7.3×10^3	0.1
2	1.8	5.5×10^3	450	100	7.0×10^3	0.03
1	1.8	4.8×10^3	440	100	6.0×10^3	0.05
0.5	1.8	2.3×10^3	430	100	2.9×10^3	0.05

The excitation efficiency can be calculated from the effective rate constant for light absorption k_A , the duration of the laser pulse t_p and the triplet quantum yield Y [3, 4]:

$$a = \frac{N_{exc}}{N_0} = 1 - e^{-k_A t_p} = 1 - e^{-\sigma_g I t_p} \quad (1)$$

where σ_g is the absorption cross section and I is the photon flux density, i.e. the photon flux per unit area. For small values of the exponent in eq. 1, $a \approx k_A t_p$. Here we estimate first $a(C_{60})$ and then use the relation $\alpha(^3C_{60}) = a(C_{60}) \cdot Y(^3C_{60})$, where $Y(^3C_{60})$ is the triplet quantum yield that is almost unity ($Y(^3C_{60}) \approx 1$) for $^3C_{60}$. [5] The photon flux density I is given by [6]:

$$I = \frac{E_{pulse}}{E_{photon} \cdot t_p \cdot \sigma} \quad (2)$$

where $E_{pulse} \approx 4$ mJ and $E_{photon} (\lambda = 532 \text{ nm}) = 3.7 \cdot 10^{-19}$ J, t_p is the duration of a laser pulse with a FWHM of 6 ns, and σ (area of the laser beam spot) $\approx 20 \text{ mm}^2$. With these parameters we obtain $I \approx 9 \cdot 10^{24}$ photons/(s·cm²). The C_{60} absorption cross section $\sigma_g(C_{60})$ is calculated from the Beer–Lambert law:

$$\sigma_g(C_{60}) = 1000 \cdot \ln(10) \cdot \frac{\varepsilon(C_{60})}{N_A} = \varepsilon(C_{60}) \cdot 3.8 \cdot 10^{-21} \text{ cm}^2 \quad (3)$$

where N_A is the Avogadro constant and ε is the extinction coefficient of C_{60} at 532nm. With $\varepsilon_{532}(C_{60}) = 750\text{-}900 \text{ M}^{-1} \text{ cm}^{-1}$ (see previous section, SI 2), $\sigma_g(C_{60})$ is $\approx 3 \times 10^{-18} \text{ cm}^2$. By inserting $\sigma_g(C_{60})$ and I into eq. 1 we finally obtain $\alpha(^3C_{60}) \approx 0.15$. This theoretical value appears to be in a reasonable agreement with the experimental values in Table 1 when considering losses of laser power during experiments (for instance, the presence of a grid in the optical window of the resonator) and through the sample concentration.

Section S4. FID intensities of the DNP ^1H -NMR measurements and pulse sequence

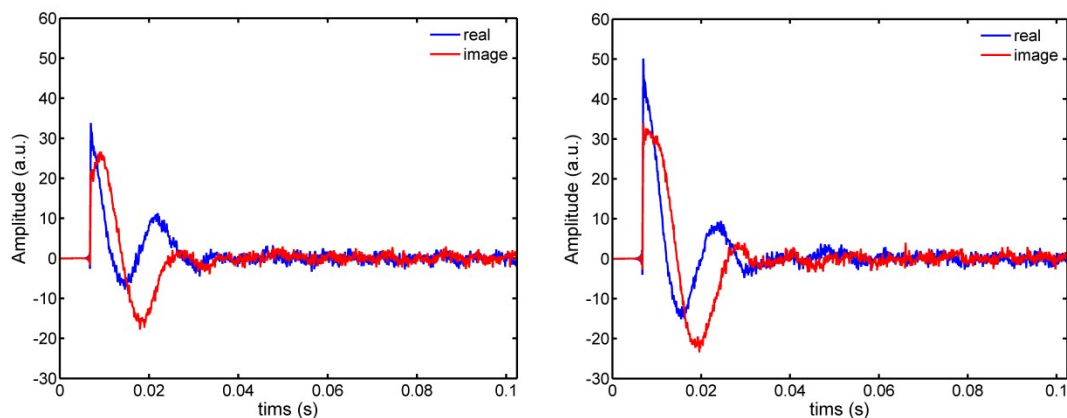


Figure S5. ^1H FID intensities (real and imaginary parts) of toluene doped with 0.8 mM **FN-1a** prior (left) and after (right) DNP with a CW 445 nm laser (3 W) and irradiation for 5 s.

References:

- 1) Rozenshtein, V.; Berg, A.; Stavitski, E.; Levanon, H.; Franco, L.; Corvaja, C., *J. Phys. Chem. A* **2005**, *109*, 11144-11154.
- 2) (a) Cataldo, F., Iglesias-Groth, S., Hafez, Y., *Eur. Chem. Bull.* **2013**, *2*(12), 1013-1018; (b) Tomiyama, T., Uchiyama, S., Shinohara, H. *Chem. Phys. Lett.* **1997**, *264*(1-2), 143-148.
- 3) Turro, N. J., *Modern Molecular Photochemistry*. University Science Books: Sausalito, 1991.
- 4) Mark Csele, *Fundamentals of light sources and lasers*, Wiley 2004, page 133.
- 5) Tomiyama, T., Uchiyama, S., Shinohara, H. *Chem. Phys. Lett.* **1997**, *264*(1-2), 143-148.
- 6) Eugene Hecht, *Optics*. 4th ed, Addison-Wesley 2002.